Physicochem. Probl. Miner. Process., 56(3), 2020, 493-503

http://www.journalssystem.com/ppmp

Physicochemical Problems of Mineral Processing

ISSN 1643-1049
© Wroclaw University of Science and Technology

Received January 31, 2020; reviewed; accepted March 30, 2020

Effect of sulfidization on the stability of adsorption of isoamyl xanthate on malachite

Kun Xiong [1], Shuming Wen [2], Zilong Liu [3], Jiushuai Deng [4], Yingbo Mao [5]

[1] College of Earth Science and Resources, Chang'an University, Xi'an 710064, China

[2] State Key Laboratory of Complex Nonferrous Metal Resources Clean Utilization, Faculty of Land Resource Engineering, Kunming University of Science and Technology, Kunming 650093, China

[3] Tibet Huatailong Mining Development Co., Ltd, China National Gold Group Corporation, Lhasa, 850200, China

[4] School of Chemical & Environmental Engineering, China University of Mining & Technology (Beijing), Beijing 100083, China

[5] Department of Metallurgy, Honghe University, Mengzi 661100, China

Corresponding authors: shmwen@126.com (S. Wen), dengshuai689@163.com (J. Deng)

Abstract: The activity and stability of adsorbed isoamyl xanthate (IX) on a malachite surface before and after sulfidization were studied by calculating the malachite dissolved component and adsorption energy and performing experiments the zeta potential measurements, adsorption and desorption, and flotation experiments. In the malachite slurry solution, the main components of copper are Cu^{2+}, $CuCO_3$, $HCuO_2^-$, CuO_2^-, and $Cu(CO_3)_2^{2-}$, and the concentration distribution of these components was related to the slurry pH value. Between pH 5 to 9, the main copper component in the slurry was $CuCO_3$. The malachite surface was negatively charged; however, the sulfur ions or hydrosulfide ions could still adsorb on the surface at a pH of more than 8.2, which indicated that the sulfidization of malachite corresponds to the chemical adsorption, and the surface electrical properties of the malachite were not obvious to the sulfidization. The adsorption activity of malachite on IX was stronger than that of the sulfide malachite; however, the desorption ratio of IX concerning the malachite was higher than that of the sulfide malachite. The adsorption energy of IX on the malachite and sulfide malachite surface was -449.6 kJ/mol and -1134.7 kJ/mol, respectively, and the IX adsorbed on the sulfide malachite surface was more stable. The flotation experiments indicated that the sulfidization of malachite reduced the consumption of IX; however, the recovery of malachite was improved.

Keywords: malachite, sulfidization, zeta potential, adsorption stability, flotation recovery

1. Introduction

In nature, copper exists mainly in the form of copper sulfide or copper oxide ores. From a global perspective, 30% of copper is extracted from copper oxide ores (Lee et al., 2009). Several different copper oxide minerals exist, and, in general, more than one is present in a deposit. The processing method of a copper oxide ore includes flotation, hydrometallurgy, and metallurgy combined processes, among which flotation is widely used because of its high efficiency, high stability, and low cost (Barbaro et al., 1997; Corin et al., 2017). Direct flotation and sulfidization-xanthate flotation are the two processes used to process a copper oxide ore. Direct flotation uses xanthate, hydroxamic acid, and sodium oleate as collectors to separate the copper oxide ores. The use of hydroxamic acid collectors has been suggested to enable the direct flotation; however, there is limited information regarding the effect of the reagent structure on the performance of these collectors (Li et al., 2015; Marion et al., 2017; Kim et al., 2019). Consequently, although the direct flotation technique is valuable, its commercial application is restrained owing to the inferior selectivity of gangue minerals.

The sulfidization-xanthate flotation of copper sulfide ore is extremely effective (Gush et al., 2005; Li

DOI: 10.37190/ppmp/119882

et al., 2014). Consequently, it is beneficial to convert a copper oxide surface into a sulfide surface and collect the copper oxide mineral with xanthate. In such a case, the sulfidization-xanthate flotation is a preferred process for the flotation of copper oxide. In this method, a sulfurizing agent is used to pre-vulcanize the copper oxide mineral, and xanthate is later used to collect the copper oxide mineral (Malghan et al., 1986). Sulfidization involves the formation of an artificial sulfidization film on the surface of the copper oxide mineral. The xanthate is adsorbed on this sulfidization film, thereby improving the hydrophobicity of the mineral surface and floating (Raghavan et al., 1984; Deng et al., 2019). Studies have shown that xanthate reacts with the copper oxide surface to form copper xanthate; however, the copper xanthate loosens and detaches owing to the weak first coating layer, leading to poor flotation recovery (Wen, 1994; Xiao et al., 2018). The theory of sulfidization flotation involves considering the adsorption of the copper oxide surface as the adsorption of the sulfide copper surface (Xu et al., 2014; Wu et al., 2015). However, in flotation experiments or even production practice, the flotation recovery of the copper oxide ore is considerably lower than that of the sulfide copper ore (Wen, 2001; Corin et al., 2017).

Interestingly, in the process of copper oxide ore flotation, the recovery of the rough concentrate is high during roughing; however, with the increase in the number of processes and the processing time, the flotation recovery drops sharply (Valdivieso, 2004; Wu et al., 2017; Liu et al., 2019). Some studies have reported that the oxidative failure of the sulfurizing agent is the main reason for the decrease in the copper oxide minerals flotation recovery (Park et al., 2016; Feng et al., 2018). The method of adding the sulfurizing agent and xanthate at different stages can obtain a better flotation effect; however, it has been noted that in practice, the flotation indicators are not considerably improved (Yu et al., 2011; Feng et al., 2016; Xu et al., 2018). Some studies indicated that a dense hydrophobic metal film is formed on the malachite surface after treatment with ammonium sulfate before sulfidization in the presence of moderate sulfidizing reagents. The addition of ammonium sulfate was noted to improve the flotation behaviour of malachite because of the formation of a dense copper sulfide film (Feng et al., 2018; Liu et al., 2018; Shen et al., 2019). Until now, research about the sulfidization flotation of copper oxide has been based on the sulfidizing mechanism and activated sulfidization. The activity and stability of the adsorbed xanthate on the malachite surface before and after sulfidization have not been extensively investigated. To this end, this study was aimed to investigate the effect of sulfidization on the stability of isoamyl xanthate (IX) adsorption on malachite by using flotation experiments and analytical techniques, including the dissolved component calculation, zeta potential measurement, adsorption and desorption experiments, and adsorption energy calculation.

2. Materials and methods

2.1. Materials

The malachite sample used for the experiments was obtained from Dongchuan in the Yunnan Province of China. The samples were crushed and ground using an agate mortar to obtain a size fraction of -75 μm + 38 μm for the flotation experiments, and finer particles sized less than 5 μm were used for the zeta potential measurements, adsorption and desorption experiments (Bo et al., 2015). The results of the X-ray diffraction analysis (D/Max 2200, Rigaku, Japan) of the malachite mineral confirmed that the malachite structure did not have any apparent impurities.

The IX and sodium sulfide provided by Hunan Minzhu Flotation Reagents Co., Ltd, were used as a collector and a sulfurizing reagent, respectively. Hydrochloric acid and sodium hydroxide of the ACS reagent grade were used to regulate the solution pH. Methyl isobutylcarbinol (MIBC) was used as a frother. Deionized (DI) water with a resistivity of 18 MΩ (Mill-Q5O, USA), was used throughout the experiments.

2.2. Methods

2.2.1. Adsorption and desorption experiments

An ultraviolet-visible spectrophotometer (UV-752, Shanghai, China) was employed to measure the absorbance of the residual agent. A total of 2 g of the sample was weighed and placed in a 200 cm^3 conical flask, and 40 cm^3 of distilled water was added. IX was added to the solution before and after the

Na_2S reagent, and the resulting sample oscillated for a different time ranging from 1 min to 30 min in an oscillator to attain equilibrium. The solution was centrifuged and filtered. Finally, the supernatant was collected for the absorbance measurement. The absorption peak at 301 nm in the UV spectrum was used for the quantitative determination of the IX. Standard solutions of 2, 4, 6, 8, and 10 mg/dm^3 IX were used to formulate the analytical calibration curve. The linear correlation coefficient was 0.9995. The relevant concentration of the residual agent was calculated using standard curves, and the adsorption of the agent on the mineral surface was later calculated from the original concentration. The adsorption of the reagent on the mineral surface was calculated as follows:

$$\Gamma = \frac{(C_0 - C)V}{m} \quad (1)$$

where Γ is the adsorption amount (mg/g), V is the solution volume (dm^3), C_0 and C are the reagent concentrations before and after adsorption (mg/dm^3), respectively, and m is the weight of the malachite (g).

After the adsorption process, the solution was centrifuged and filtered as much as possible to obtain the adsorbent. Next, the adsorbent was placed in a 200 cm^3 conical flask, and 40 cm^3 of deionized water was added to it. This solution oscillated for 2 min in the oscillator. After the desorption process, the solution was centrifuged and filtered as much as possible to obtain the filtrate. The absorbance measurement was performed to determine the desorption of the reagent on the mineral surface of the IX in the filtrate. All adsorption and desorption amount results presented were an average of duplicate adsorption and desorption experiments.

2.2.2. Zeta potential measurements

The zeta potential measurements were carried out using a ZetaProbe instrument (Colloidal Dynamics Company, USA). In each experiment, the malachite sample was placed in a measuring cup filled with DI water, and the concentration of the sample solution was 5% (Feng et al., 2020). The pH of the solution was adjusted by adding HCl solution (2 mol/dm^3) and NaOH solution (2 mol/dm^3). Subsequently, the zeta potentials of the malachite surface were measured on a Zeta Probe potentiometer in the presence and absence of Na_2S.

2.2.3. Flotation experiments

Flotation experiments were performed on two groups: Experiments on the group were performed without adding Na_2S in the solution, and those on the other group involved the addition of Na_2S. Pure malachite mineral (2 g) and DI water (40 cm^3) were mixed in a Plexiglas cell. The pulp pH was adjusted to 9.0 by added NaOH or/and HCl, and a freshly prepared Na_2S solution with the desired dosage was added to sulfidize the malachite surface for 3 min. The collector IX and MIBC were added sequentially into the suspension and conditioned for 3 min and 1 min, respectively. The flotation was conducted for 5 min. Subsequently, the float and sink were filtered, dried, and weighed to calculate the flotation recovery. All recovery results are an average of duplicate flotation experiments.

2.2.4. Adsorption energy calculation

The adsorption energy of malachite and sulfurized malachite with IX was calculated using the CASTEP module of Materials Studio 8.0 (Segall et al., 2002). The generalized gradient approximation technique using the PBE functional for solids was used to approximate the exchange-correlation energy. Ultrasoft pseudopotentials were used to describe the interaction between the valence electrons and the ionic core (Kresse et al., 1999; Deng et al. 2019). The considered valence electron configurations of malachite were Cu $3d^{10}4s^1$, C $2s^22p^2$, O $2s^22p^4$, and H $1s^1$. The valence electron configurations of the IX were C $2s^22p^2$, O $2s^22p^4$, S $3s^23p^4$, and H $1s^1$. The optimal cut-off kinetic energy was 351 eV, based on the test results, and the BFGS method was utilized to optimize the atomic positions. The malachite (201) surface was chosen as a surface model for the adsorption calculations in this study, as it is the most stable surface of malachite and facilitates the adsorption of the flotation reagents.

The adsorption energy of the IX molecule that adsorbed onto the malachite (201) surface and sulfurized malachite (201) surface were calculated according to Eq. (2) and Eq. (3), respectively:

$$\Delta E_{ads} = E_{malathite+IX} - E_{malachite} - E_{IX} \quad (2)$$

$$\Delta E_{ads} = E_{sulfurized\ malathite+IX} - E_{malachite} - E_{IX} - E_{sulfurized\ malachite} \quad (3)$$

where ΔE_{ads} represents the adsorption energy, $E_{malathite+IX}$ represents the total energy of the malachite surface with the IX molecule adsorbed, $E_{malachite}$ represents the total energy of the reconstructed malachite surface, E_{IX} represents the total energy of the IX molecule before adsorption onto the mineral surface, $E_{sulfurized\ malathite+IX}$ represents the total energy of the sulfurized malachite surface with the IX molecule adsorbed, and $E_{sulfurized\ malachite}$ represents the total energy of the sulfurized malachite surface. The additional negative adsorption energy indicated an increasingly strong interaction between the IX molecule and the malachite surface.

3. Results and discussion

3.1. Effect of pH on the composition of the malachite solution

Malachite is a sparingly soluble copper carbonate-hydroxide mineral (Oprea et al., 2004). In solution, parts of cupric, carbonate, and hydroxyl ions are dissolved from the malachite surface. Therefore, they are the common ions of malachite, which can affect the solubility of malachite and thus the flotation performance (Du et al., 1997; Feng et al., 2017).

The sulfidization and adsorption performances are influenced by the dissolution of the malachite surface and various components in the slurry solution, and the pH of the solution directly determines the distribution of the concentration of these components (Chen et al., 2020). The malachite surface is hydrolyzed by the polar water molecules on an aqueous solution. Cu^{2+}, $Cu(CO_3)$, $Cu(CO_3)_2^{2-}$, $HCuO_2^-$, CuO_2^{2-}, $Cu(OH)^+$, $Cu(OH)_2$, $Cu_2(OH)_2^{2+}$, $Cu(OH)_3^-$, $Cu(OH)_4^{2-}$, H_2CO_3, HCO_3^-, and CO_3^{2-} are the possible components in the solution. The chemical reactions and their equilibrium equations of $Cu_2(OH)_2CO_3$-H_2O in the system are presented in Table 1.

Table 1. Chemical reactions and equilibrium equations of $Cu_2(OH)_2CO_3$-H_2O system (25 °C)

Chemical reactions	logK	Equilibrium equations of log[HCO_3^-]=-2
$Cu_2(OH)_2CO_3+2H_2O=2HCuO_2^-+HCO_3^-+3H^+$	-48.88	Log[$HCuO_2^-$] = -23.44+3/2pH
$Cu_2(OH)_2CO_3+2H_2O=2CuO_2^-+HCO_3^-+5H^+$	-75.76	Log[CuO_2^-] = -36.88+5/2pH
$Cu_2(OH)_2CO_3+3H^+=2Cu^{2+}+HCO_3^-+2H_2O$	4.54	Log[Cu^{2+}] = 3.27-3/2pH
$Cu_2(OH)_2CO_3+HCO_3^-+H^+=2CuCO_3+2H_2O$	-2.62	Log[$CuCO_3$] = -2.31-1/2pH
$Cu_2(OH)_2CO_3+3HCO_3^-=2Cu(CO_3)_2^{2-}++2H_2O+H^+$	-16.85	Log[$Cu(CO_3)_2^{2-}$] = -11.42+1/2pH

Studies have reported that copper exists in five forms after malachite dissolves in water, i.e., Cu^{2+}, $Cu(CO_3)$, $HCuO_2^-$, CuO_2^-, and $Cu(CO_3)_2^{2-}$. Based on mass conservation, the total concentration of copper in the solution can be expressed as in Eq. (4):

$$[Cu_T] = [Cu^{2+}] + [CuCO_3] + [HCuO_2^-] + [CuO_2^-] + [Cu(CO_3)_2^{2-}] \quad (4)$$

The substitution of the five forms of copper concentration in Eq. (5) gives the following expression:

$$[Cu_T] = 10^{4.54/2}[H^+]^{3/2}[HCO_3^-]^{-1/2}+10^{2.62/2}[H^+]^{1/2}[HCO_3^-]^{1/2}+10^{-48.88/2}[H^+]^{-3/2}[HCO_3^-]^{-1/2} +10^{-75.76/2}[H^+]^{-5/2}[HCO_3^-]^{-1/2}+10^{-16.85/2}[H^+]^{-1/2}[HCO_3^-]^{3/2} \quad (5)$$

The substitution of the equilibrium equations in Eq. (6) yields:

$$[Cu_T] = 10^{3.27}[H^+]^{1.5}+10^{-2.31}[H^+]^{0.5}+10^{-23.44}[H^+]^{-1.5}+10^{-36.88}[H^+]^{-4.5}+10^{-11.42}[H^+]^{-0.5} \quad (6)$$

In the equations below, the α_1, α_2, α_3, α_4, and α_5 represent the percentages of Cu^{2+}, $CuCO_3$, $HCuO_2^-$, CuO_2^-, and $Cu(CO_3)_2^{2-}$, respectively. Therefore, the percentage of each component in the aqueous solution can be expressed as:

$$\alpha_1 = [Cu^{2+}]/[Cu^T] = 10^{3.27}[H^+]^{1.5}/[Cu_T] \quad (7)$$

$$\alpha_2 = [CuCO_3]/[Cu^T] = 10^{-2.31}[H^+]^{0.5}/[Cu_T] \quad (8)$$

$$\alpha_3 = [HCuO_2^-]/[Cu^T] = 10^{-23.44}[H^+]^{-1.5}/[Cu_T] \quad (9)$$

$$\alpha_4 = [CuO_2^-]/[Cu^T] = 10^{-36.88}[H^+]^{-4.5}/[Cu_T] \quad (10)$$

$$\alpha_5 = [Cu(CO_3)_2^{2-}]/[Cu^T] = 10^{-11.42}[H^+]^{-0.5}/[Cu_T] \quad (11)$$

The above equations show that the forms of copper present in the aqueous solution are closely related to the pH value of the solution. The percentages of Cu^{2+}, $CuCO_3$, $HCuO_2^-$, CuO_2^-, and $Cu(CO_3)_2^{2-}$ in the solution can, therefore, be obtained. Fig. 1 shows the distribution of the forms of copper components in the solution at different pH values after the dissolution of malachite. At pH < 7, the copper in the solution exists as Cu^{2+} and $CuCO_3$. At 7 < pH < 10, the content of $CuCO_3$ in the solution gradually decreases, and the content of $Cu(CO_3)_2^{2-}$ increases continuously, which becomes the main form of copper in the solution. At 10 < pH < 12, the content of $Cu(CO_3)_2^{2-}$ decreases, whereas the content of $HCuO_2^-$ increases with the increase in the pH value. At pH > 12, the dissolved components of malachite mainly include $Cu(CO_3)_2^{2-}$, $HCuO_2^-$, and CuO_2^{2-}. With the increase in the pH, the content of CuO_2^{2-} continuously increases, whereas the content of $Cu(CO_3)_2^{2-}$ decreases, and the content of $HCuO_2^-$ first increases and then decreases. The relationship between the copper concentration in the malachite slurry solution and pH value indicates that the forms of copper in the solution change with the pH value (Luo et al., 2019). The change in the composition of the solution affects the surface properties, adsorption, and flotation of the malachite. It can be predicted that when the pH of the slurry is between 8 and 9, because $Cu(CO_3)$ is the dominant component in the slurry solution, the mineral surface potential is close to zero point. When the pulp pH is less than 8, the mineral surface is positively charged, and when the pH range of the pulp is greater than 9, the surface potential of the mineral is negative. The solubility of the malachite decreases sharply with the increase in the pH from 3 to 8.2 and reaches its minimum value at a pH of approximately 8.2. Above this pH value, the solubility increases with a further increase in the pH (Li et al., 2019). The ions near the zero point in the slurry solution are the localized ions on the surface of the malachite.

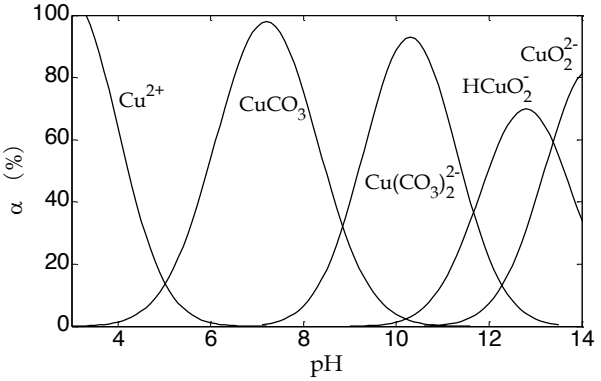

Fig. 1. Effect of pH value on the content of dissolved components of malachite

3.2. Zeta potential measurements

Fig. 2 shows the zeta potentials of the malachite in the presence and absence of Na_2S as a function of the pH. In the absence of Na_2S, the isoelectric point (IEP) of malachite was found to be pH 8.2, which is in agreement with the findings reported in literature (Liu et al., 2016). In the presence of Na_2S, the IEP of malachite became more negative, and the IEP changed to 7.0. The addition of Na_2S decreased the zeta potential values over the entire pH range because the S^{2-} and HS^- produced by the hydrolysis of Na_2S reacted with the copper ions on the malachite surface to form a copper-sulfur compound, which further reduced the electronegativity of the mineral surface, thereby indicating the chemical adsorption of S^{2-} and HS^- on the malachite surface.

3.3. Effect of sodium sulfide on the adsorption and desorption of IX

The adsorption of IX on the malachite surface was determined before and after the addition of Na_2S, and the results are shown in Fig. 3. As seen in Fig. 3, IX adsorbed on both the malachite and sulfide malachite surface, and the saturated adsorption amounts were 7.8 mg/g and 7.3 mg/g after stirring for 3 min, respectively. The amount of saturated adsorption of the IX on the malachite surface was higher than that on the sulfide malachite surface, indicating that the malachite surface had a higher adsorption activity about the IX than the sulfide malachite surface. After stirring for 24 min, the adsorption amounts were stable at 2.8 mg/g and 5.3 mg/g on the malachite and sulfide malachite surface, respectively. With

the increase in the stirring time, the adsorption amount of IX on the malachite surface desorbed faster than that on the sulfide malachite surface; in other words, the desorption rate of IX on the malachite was faster than that on sulfide malachite surface. This indicates that the sulfidization of malachite reduces the adsorption amount and adsorption activity of the malachite to the IX; however, the sulfidization of the malachite enhances the adsorption strength and stability.

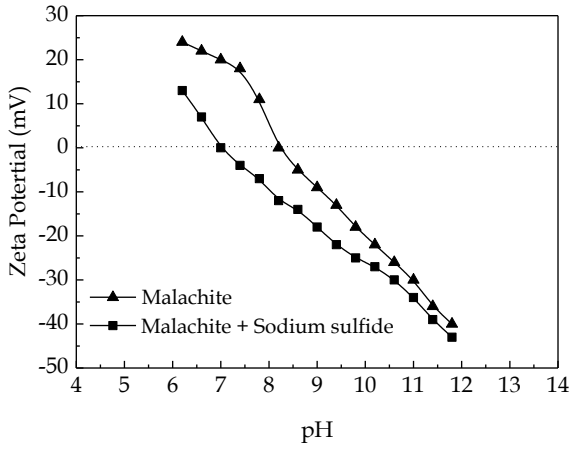

Fig. 2. Effect of pH value on zeta potential of malachite

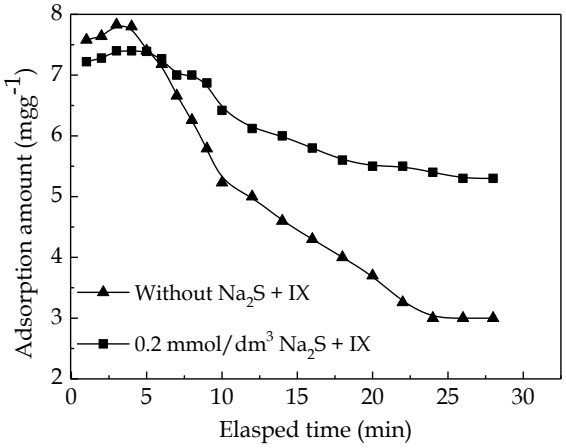

Fig. 3. Effect of stirring time on adsorption amount of IX on malachite and sulfide malachite surface

The malachite and sulfide malachite surface were washed several times after the adsorption of the IX was saturated, and the desorption ratio of the IX on the malachite and sulfide malachite surfaces was determined. As shown in Fig. 4, the desorption ratio of IX adsorbed on the malachite surface was 17.5%

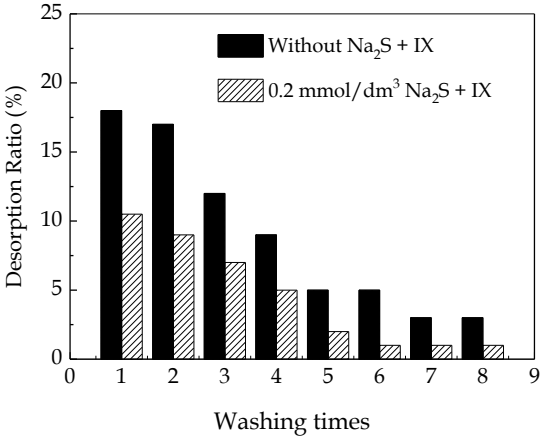

Fig. 4. Effect of washing times on desorption ratio of IX on malachite and sulfide malachite surface

after the first washing, and the desorption ratio after the second and third washing was 14.5% and 11.2%, respectively. The total desorption ratio of IX adsorbed on the malachite surface was 67.3% after eight washes. However, the total desorption ratio of IX adsorbed on the sulfide malachite surface was only 35.4%. The results showed that the desorption mount of IX on the sulfide malachite surface was considerably smaller than that on the malachite surface. The process of sulfidization could inhibit the desorption of IX on the sulfide malachite surface, and the adsorption of IX on sulfide malachite surface was stronger. In other words, the process of sulfidization improved the stability of the IX adsorption layer.

3.4. Calculation of adsorption energy of IX on malachite surface

Fig. 5 shows the configuration of the IX molecule adsorbed at the top Cu site onto the malachite (201) surface. As shown in Fig. 5, the IX molecule adsorbed vertically on the surface of the malachite (201). Two stable adsorption configurations were present: One was the single bond S1 in the IX molecule adsorbed at the top Cu site onto the malachite (201) surface, which was recorded as the top-IX-S1 configuration (Fig. 5 (a)); the other included the single bond S1 atom and the double bond S2 atom in the IX molecule adsorbed at the top Cu site onto the malachite (201) surface, which was recorded as the top-IX-S1S2 (Fig. 5 (b)). In the two adsorption configurations, the hydrophobic group part of IX was located at the outermost end, and the solid affinity group interacted with the Cu atom on the surface of the malachite. The adsorption of IX influenced the secondary structure of the malachite crystal. A certain interaction occurred between the Cu and O atoms between the first and secondary layers. The adsorption energy of IX on the top-IX-S1 and top-IX-S1S2 on the malachite (201) surface was -437.10 kJ/mol and -449.64 kJ/mol, respectively, indicating that the IX molecule can adsorb on the malachite (201) surface.

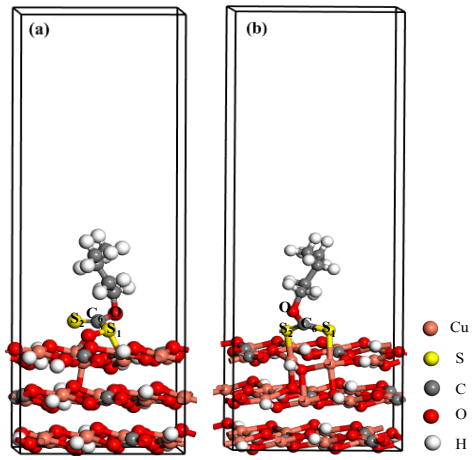

Fig. 5. Adsorption configurations of IX molecule on malachite (201) surface: (a) Top-IX-S_1 absorption, (b) Top-IX-S_1S_2 absorption

Fig. 6 shows the configuration of the IX molecule adsorbed at the top Cu site onto the sulfide malachite (201) surface. It can be seen from Fig. 6 that the single bond S1 in the IX molecule adsorbed at the top Cu site onto the sulfide malachite (201) surface, and a certain interaction occurred between the Cu atom and O atom in the adjacent layer. The adsorption of the IX molecule not only affected the secondary structure of the sulfide malachite crystal, but also affected the third layer. Previous studies have confirmed the interlayer sulfidization of malachite (Wu et al., 2017). After sulfidization occurs, the adjacent layers contribute to the stability of the overall structure of malachite and sulphide malachite crystal. Compared with the IX molecule adsorbed directly onto the malachite surface, the configuration of the IX molecule on the sulfide malachite surface was more stable in structure. The adsorption energy of the IX molecule at the Cu site on the sulfide malachite (201) surface was -1134.72 kJ/mol. The presence of negative adsorption energy suggests that the IX molecule can spontaneously react with the sulfide malachite (201) surface, and the adsorption energy is more negative than that of IX molecule directly on the malachite (201) surface (-449.64 kJ/mol). These results demonstrate that the adsorption stability of the IX molecule on the sulfide malachite (201) surface is stronger than that of IX molecule on the

malachite (201) surface, and IX molecule more favorably adsorbs on the sulfide malachite (201) surface.

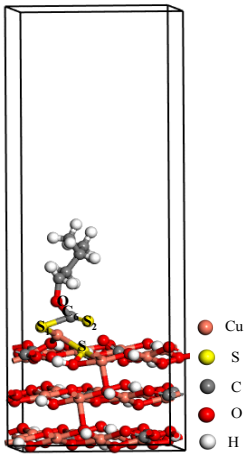

Fig. 6. Adsorption configurations of the IX molecule on sulfurized malachite (201) surface

3.5. Flotation experiments

The recovery of the malachite and sulfide malachite under different stirring time conditions is shown in Fig. 7. It can be seen from Fig. 7 that both the malachite and sulfide malachite could float using IX as the collector, and the flotation recoveries were 41.0% and 47.2% after stirring for 3 min, respectively. At a stirring time of 21 min, the recovery of the malachite and sulfide malachite decreased to 20.3% and 38.3%, respectively. The flotation recovery of the sulfide malachite was higher than that of the malachite throughout the stirring time. With the increase in the stirring time, the floating recovery of the malachite decreased rapidly, while the recovery of the sulfide malachite decreased slowly, indicating that the hydrophobicity of the malachite surface reduced faster than that of the sulfide malachite surface. The sulfidization enhanced the stability of the adsorption of IX on the surface of malachite, as directly reflected by the recovery of the mineral flotation.

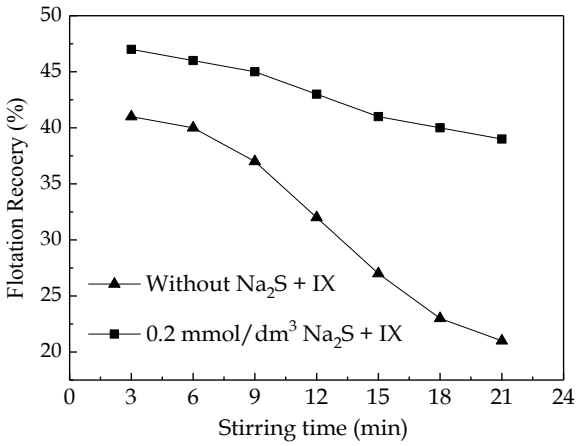

Fig. 7. Effect of stirring time on flotation recovery of malachite and sulfide malachite

When the collector of the IX interacts with the malachite surface, the xanthate ions mainly replace the CO_3^{2-} and OH^- on the malachite surface to form copper xanthate. As the reaction activity of malachite surface is higher than that of the sulfide malachite, the adsorption capacity of IX on the malachite surface is higher than that of the sulfide malachite; however, the adsorption layer of copper xanthate on the malachite surface is unstable and easily detaches, which results in the low recovery of malachite flotation.

When the collector of IX interacts with the surface of the sulfide malachite, the existence of sulfur ions in the pulp and the sulfide ions formed on the surface of the sulfide malachite can restrict the adsorption of IX on the surface of the sulfide malachite. Therefore, the adsorption activity of the sulfide

malachite to IX decreases, and the adsorption capacity reduces. However, the desorption tests and flotation experiments indicate that the stability of the adsorbed IX is enhanced, and the recovery of flotation is improved. In the process of the sulfurization flotation of the malachite, the occurrence of sulfurization reduces the adsorption activity of the sulfide malachite to IX; however, the stability of the IX adsorption layer is improved, and the flotation recovery is improved.

4. Conclusions

The chemical calculation results showed that the main component of copper in malachite slurry solution was Cu^{2+}. The concentration distribution of the components $CuCO_3$, $HCuO_2^-$, CuO_2^-, and Cu $(CO_3)_2^{2-}$ varied with the pH value of the slurry. When the pH was greater than the malachite zero point of 8.2, the negatively charged sulfur or sulfur ions could still adsorb on the malachite surface, indicating that the sulfidization of malachite corresponded to chemical adsorption. The adsorption capacity of IX on malachite was higher than the sulfide malachite surface. The occurrence of sulfidization reduced the adsorption activity of sulfide malachite to IX. The adsorption energy of the IX molecule on malachite and sulfide malachite was calculated as -449.60 kJ/mol and -1134.72 kJ/mol, respectively. The negative adsorption energy suggested that IX molecule could react with sulfide malachite, and adsorption stability of IX molecule on sulfide malachite was higher than the malachite surface. The flotation recovery of sulfide malachite was higher than malachite due to the improved stability of the IX adsorption layer. The results of zeta potential, adsorption and desorption experiments and adsorption energy are in good agreement with flotation experiments. In conclusion, the sulfidization reduced the adsorption activity of sulfide malachite to IX but enhanced the stability of the adsorption of IX on the surface of sulfide malachite.

Acknowledgments

This research project was supported by the National Natural Science Foundation of China (51764022), Fok Ying Tong Education Foundation (161046), China Postdoctoral Science Foundation (2018M632810), and Supported by the Fundamental Research Funds for the Central Universities, CHD (300102270105).

References

BARBARO, M., URBINA, R.H., COZZA, C., FUERSTENAU, D., MARABINI, A., 1997. *Flotation of oxidized minerals of copper using a new synthetic chelating reagent as collector*. International Journal of Mineral Processing, 50, 275-287.

BO, F., LUO, X.P., WANG, J.Q., WANG, P.C., 2015. *The flotation separation of scheelite from calcite using acidified sodium silicate as depressant.* Minerals Engineering, 80, 45-49.

CHEN, B., BAO, S.X., ZHANG, Y.M., 2020. *Column separation of vanadium(v) from complex sulfuric solution using trialkylamine-impregnated resins.* JOM, 72, 953-961.

CORIN, K.C., KALICHINI, M., O'CONNOR, C.T., SIMUKANGA, S., 2017. *The recovery of oxide copper minerals from a complex copper ore by sulphidisation.* Minerals Engineering, 102, 15-17.

DENG, J., LAI, H., WEN, S., & LI, S., 2019. *Confirmation of Interlayer Sulfidization of Malachite by TOF-SIMS and Principal Component Analysis.* Minerals, 9(4), 204-214.

DENG, J., LAI, H., CHEN, M., GLEN, M., WEN, S., ZHAO, B., LIU, Z., HUA, Y., LIU, M., HUANG, L., GUAN, S., YANG, P., 2019. *Effect of iron concentration on the crystallization and electronic structure of sphalerite/marmatite: A DFT study.* Minerals Engineering, 136, 168-174.

DU, Q., SUN, Z.X., FORSLING, W., TANG, H.X., 1997. *Adsorption of copper at aqueous illite surfaces.* Journal of Colloid and Interface Science, 187, 232-242.

FENG, B., ZHONG, C., ZHANG, L., GUO, Y., WANG, T., HUANG, Z., 2020. *Effect of surface oxidation on the depression of sphalerite by locust bean gum.* Minerals Engineering, 146, 106-142.

FENG, Q.C., WEN, S.M., ZHAO, W.J., DENG, J.S., XIAN, Y.J., 2016. *Adsorption of sulfide ions on cerussite surfaces and implications for flotation.* Applied Surface Science, 360, 365-372.

FENG, Q.C., ZHAO, W.J., WEN, S.M., 2018a. *Surface modification of malachite with ethanediamine and its effect on sulfidization flotation.* Applied Surface Science, 436, 823-831.

FENG, Q.C., ZHAO, W.J., WEN, S.M., 2018b. *Ammonia modification for enhancing adsorption of sulfide species onto*

malachite surfaces and implications for flotation. Journal of Alloys and Compounds, 744, 301-309.

FENG, Q.C., ZHAO, W.J., WEN, S.M., CAO, Q.B., 2017. *Copper sulfide species formed on malachite surfaces in relation to flotation.* Journal of Industrial and Engineering Chemistry, 48, 125-132.

GUSH J.C.D., 2005. *Flotation of oxide minerals by sulphidization–the development of a sulphidization control system for laboratory testwork.* Journal of the South African Institute of Mining and Metallurgy, 105, 193-197.

KIM, H., YOU, J., GOMEZ FLORES, A., SOLONGO, S.K., HWANG, G., ZHAO, H.B., LEE, B.C., CHOI, J., 2019. *Malachite flotation using carbon black nanoparticles as collectors: Negative impact of suspended nanoparticle aggregates.* Minerals Engineering, 137, 19-26.

KRESSE, G., JOUBERT, D., 1999. *From ultrasoft pseudopotentials to the projector augmented-wave method.* Physical Review B, 59(3), 1758-1775.

LEE, K., ARCHIBALD, D., MCLEAN, J., REUTER, M.A., 2009. *Flotation of mixed copper oxide and sulphide minerals with xanthate and hydroxamate collectors.* Minerals Engineering, 22, 395-401.

LI, C.X., WEI, C., DENG, Z.G., LI, X.B., LI, M.T., XU, H.S., 2014. *Hydrothermal sulfidation and flotation of oxidized zinc–lead ore.* Metallurgical and Materials Transactions B, 45, 833-838.

LI, F.X., ZHONG, H., XU, H.F., JIA, H., LIU, G.Y., 2015. *Flotation behavior and adsorption mechanism of a-hydroxyoctyl phosphinic acid to malachite.* Minerals Engineering, 71, 188-193.

LI, Z.L., RAO, F., SONG, S.X., URIBE-SALAS, A., LOPEZ-VALDIVIESO, A., 2019. *Effects of common ions on adsorption and flotation of malachite with salicylaldoxime.* Colloids and Surfaces A, 577, 421-428.

LIU, C., FENG, Q.M., ZHANG, G.F., 2018. *Effect of ammonium sulfate on the sulfidation flotation of malachite.* Archives of Mining Sciences, 63, 139-148.

LIU, C., SONG, S.X., LI, H.Q., AI, G.H., 2019. *Sulfidization flotation performance of malachite in the presence of calcite.* Minerals Engineering, 132, 293-296.

LIU, G.Y., HUANG, Y.G., QU, X.Y., XIAO, J.J., YANG, X.L., XU, Z.H., 2016. *Understanding the hydrophobic mechanism of 3-hexyl-4-amino-1, 2,4-triazole-5-thione to malachite by ToF-SIMS, XPS, FTIR, contact angle, zeta potential and micro-flotation.* Colloids and Surfaces A, 503, 34-42.

LUO, Y.P., BAO, S.X., ZHANG, Y.M., 2020. *Preparation of one-part geopolymeric precursors using vanadium tailing by thermal activation.* Journal of the American Ceramic Society, 103(2), 779-783.

MALGHAN, S.G., 1986. *Role of sodium sulfide in the flotation of oxidized copper, lead, and zinc ores.* Minerals and Metallurgical Processes, 3, 158-163.

MARION, C., JORDENS, A., LI, R.H., RUDOLPH, M., WATERS, K.E., 2017. *An evaluation of hydroxamate collectors for malachite flotation.* Separation and Purification Technology, 183, 258-269.

OPREA, G., MIHALI, C., DANCIU, V., PODARIU, M., 2004. *The Study of 8-hydroxyquinoline and salicylaldoxime action at the malachite flotation.* Journal of Mining and Metallurgy, 40, 49-63.

PARK, K., PARK, S., CHOI, J., KIM, G., TONG, M., KIM, H., 2016. *Influence of excess sulphide ions on the malachite-bubble interaction in the presence of thiol-collector.* Separation and Purification Technology, 168, 1-7.

SEGALL, M.D., LINDAN, P.J., PROBERT, M.A., PICKARD, C.J., HASNIP, P.J., CLARK, S.J., PAYNE, M.C., 2002. *First-principles simulation: ideas, illustrations and the CASTEP code.* Journal of Physics: Condensed Matter, 14(11), 2717-2744.

SHEN, P.L., LIU, D.W., ZHANG, X.L., JIA, X.D., SONG, K.W., LIU, D., 2019. *Effect of $(NH_4)_2SO_4$ on elimination the depression of excess sulfide ions in the sulfidization flotation of malachite.* Minerals Engineering, 137, 43-52.

RAGHAVAN, S., ADAMEC, E., LEE, L., 1984. *Sulfidization and flotation of chrysocolla and brochantite.* International Journal of Mineral Processing, 12, 173-191.

VALDIVIESO, 2019. *Effects of common ions on adsorption and flotation of malachite with salicylaldoxime.* Colloids and Surfaces A, 577, 421-428.

WEN, S.M., 1994. *A study on the stability of collector adsorption layers on copper and zinc mineral surfaces.* Journal of Kunming University of Science and Technology, 19 (3), 131-134.

WEN, S.M., 2001. *Research test on stability of xanthate layer absorbed onto surface of malachite.* China Mining Magazine, 10, 58-60.

WU, D.D., MAO, Y.B., DENG, J.S., WEN, S.M., 2017. *Activation mechanism of ammonium ions on sulfidation of malachite (-201) surface by DFT study.* Applied Surface Science, 410, 126-133.

WU, D.D., WEN, S.M., DENG, J.S., LIU, J., MAO, Y.B., 2015. *Study on the sulfidation behaviour of smithsonite.* Applied Surface Science, 329, 315-320.

XIAO, J.J., LIU, G.Y., ZHONG, H., 2018. *Hydrophobic mechanism of N-butoxypropyl-S-(2-(hydroxyimino) propyl)*

dithiocarbamate ester to malachite flotation. The Chinese Journal of Nonferrous Metals, 28(2), 53-61.

XU, H.F., CHEN, W., ZHONG, H., HUANG, W.P., DAI, K., 2018. *Flotation behavior and adsorption mechanism of C8-chain alkyl hydroxamic acid to malachite.* The Chinese Journal of Nonferrous Metals, 28, 189-198.

XU, H.F., ZHONG, H., WANG, S., NIU, Y.N., LIU, G.Y., 2014. *Synthesis of 2-ethyl-2-hexenal oxime and its flotation performance for copper ore.* Minerals Engineering, 66-68, 173-180.

YU, J., YANG, H.Y., FAN, Y.J., 2011. *Effect of potential on characteristics of surface film on natural chalcopyrite.* Transactions of Nonferrous Metals Society of China, 21(8), 1880-1886.